CHAPTER 2

THERMOELASTIC DAMPING ANALYSIS IN MICRO AND NANOBEAM RESONATORS BASED ON HEAT CONDUCTION MODEL WITH A SINGLE DELAY TERM

2.1 Analysis of the Quality Factor of Microbeam Resonators Based on Heat Conduction Model with a Single Delay Term

2.1.1 Introduction[1]

The thermoelastic damping (TED) in micro and nanomechanical systems are interesting and challenging area of research in recent years. Prediction of TED is more challenging under the effect of non-Fourier heat conduction. As discussed in the previous chapter, several works have been dedicated to TED modeling with the influence of non-Fourier heat conduction in view of the fact that non-Fourier heat conduction model is more relevant for analysis of TED for small-scale devices. The present chapter focuses on the analysis of thermoelastic damping (TED) in micro and nanobeam resonators with the help of the quality factor in the context of thermoelastic heat conduction model

[1]The content of this sub chapter is published in ***Journal of Thermal Stresses***, 42.8 (2019):929-942.

with a single delay term. This chapter is divided into two different subchapters. The first subchapter (2.1) discusses the results of TED for microbeam resonators, whereas the second subchapter (2.2) presents the analysis of TED in nanobeam resonators by employing the recently proposed thermoelasticity theory given by Quintanilla (2011). The problem is solved by using two different approaches in two subchapters.

In subchapter 2.1, TED in microbeam resonators is investigated by following frequency approach method as reported by Lifshitz and Roukes (2000). The amount of TED in terms of the inverse quality factor is reported as $Q^{-1} = 2\left|Im\left(\omega\right)\right| / \left|Re\left(\omega\right)\right|$. Here, the real part $Re\left(\omega\right)$ of frequency ω gives the new eigenfrequencies of the beam in the presence of thermoelastic coupling and the imaginary part $\left|Im\left(\omega\right)\right|$ gives the attenuation of the vibration. It is worth mentioning here that the phenomena of TED was first observed by Zener (1937; 1938). By employing the classical Fourier heat conduction theory, he derived an expression of the quality factor for microbeam. Thereafter, Lifshitz and Roukes (2000) extended the Zener's work and developed a closed form expression of the quality factor in microbeam resonators. They analyzed that the energy dissipation of micro resonators increases significantly with the decrease of size of the beam, even when it is made with the pure single crystal materials. The TED in nanomechanical resonators has been studied by Khisaeva and Ostoja-Starzewski (2006) using generalized thermoelasticity theory with one relaxation time proposed by Lord and Shulman (1967). The different affective factors on TED such as the height of the microbeam, relaxation time, and aspect ratio between the temperature rise and thermal expansion based on dual-phase-lag (DPL) thermoelasticity theory was analyzed by Guo et al. (2012). Youssef and Alghamdi (2015) also discussed TED in rotating rings by using dual-phase-lag generalized thermoelasticity theory. Kumar et at. (2018) revealed the investigation of TED in micromechanical resonators based on thermoelastic theory with three-phase-lagging effect proposed by Roychoudhuri (2007).

In this section of the thesis, microbeam resonator is considered to analyze TED in the context of thermoelastic heat conduction model with a single delay term (Quintanilla, 2011). The equation of motion of the microbeam is derived considering Euler-Bernoulli beam theory. Moreover, the unified equation of motion is derived based on four different thermoelastic models; Lord-Shulman (LS) model, Green-Naghdi (GN-III) model, three-phase-lag (TPL) model, and new model with a single delay term. An expression of the quality factor for TED has been derived in unified form, and the variation of TED with respect to normalized frequency and the microbeam thickness has been studied. The complex frequency approach is used to analyze TED of microbeam resonator's sensitivity. The impact of the four models as mentioned above on TED is analyzed in a detailed manner.

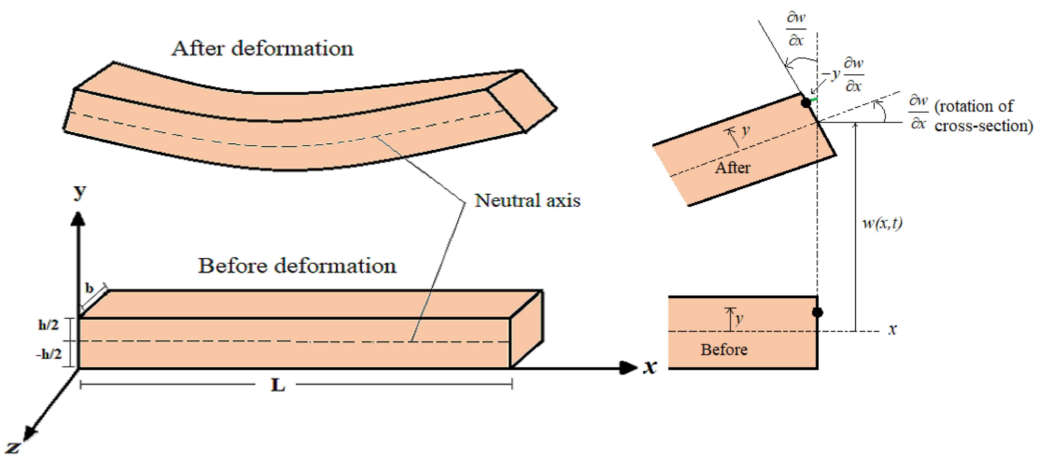

Figure 2.1.1: Deformation of an Euler-Bernoulli beam.

2.1.2 Problem formulation

We consider a problem of TED in an isotropic and homogeneous medium of microbeam resonator. For this, let us assume that there be small flexural deflections of a thin elastic microbeam with dimensions of length $L\,(0 \le x \le L)$, width $b\,(-b/2 \le z \le +b/2)$ and thickness $h\,(-h/2 \le y \le +h/2)$. We consider the x-axis along the axis of the beam, y

and z-axes corresponding to the thickness and width, respectively. In equilibrium, it is assumed that the beam resonator is unstressed and unstrained at ambient temperature T_0 everywhere.

According to the Euler-Bernoulli beam theory, the components of strain tensor and volumetric strain are given by (Lifshitz and Roukes, 2000; Guo et al., 2012)

$$\begin{aligned} \epsilon_{xx} = -y\frac{\partial^2 w}{\partial x^2}, \quad \epsilon_{yy} = \epsilon_{zz} = \nu y\frac{\partial^2 w}{\partial x^2} + (1+\nu)\,\alpha_T\theta \\ \epsilon = \epsilon_{xx} + \epsilon_{yy} + \epsilon_{zz} = (2\nu - 1)\,y\frac{\partial^2 w}{\partial x^2} + 2\,(1+\nu)\,\alpha_T\theta \end{aligned} \tag{2.1.1}$$

Also, the equation of motion based on Euler-Bernoulli beam theory with thermoelastic coupling effect is given by (Lifshitz and Roukes, 2000; Guo et al., 2012)

$$EI\frac{\partial^4 w}{\partial x^4} + E\alpha_T\frac{\partial^2 M_T}{\partial x^2} + \rho A\frac{\partial^2 w}{\partial t^2} = 0 \tag{2.1.2}$$

where EI is the flexural rigidity and A is the cross-section area of the beam. The moment of inertia I and the thermal moment M_T are expressed by

$$I = \int_A y^2 dA, \quad M_T = \int_A y\theta dA \tag{2.1.3}$$

Here, $\theta = T - T_0$ denotes the temperature increment from reference temperature T_0.

2.1.3 Unified heat conduction equation

Lord and Shulman (1967) proposed a thermoelastic model in which the heat conduction law is reacquired by the following Cattaneo-Vernotte (1958, 1961) heat conduction model in which one thermal relaxation time parameter is included:

$$q(\boldsymbol{r}, t) + \tau_q \dot{q}(\boldsymbol{r}, t) = -k\nabla T(\boldsymbol{r}, t) \tag{2.1.4}$$

Green and Naghdi heat conduction equation of type III (GN-III) is given by

$$q\left(\boldsymbol{r},t\right)=-\left[k\nabla T\left(\boldsymbol{r},t\right)+k^{*}\upsilon\left(\boldsymbol{r},t\right)\right] \tag{2.1.5}$$

in which $\dot{\upsilon}=T$. The TPL heat conduction equation is given by

$$q\left(\boldsymbol{r},t+\tau_{q}\right)=-\left[k\nabla T\left(\boldsymbol{r},t+\tau_{T}\right)+k^{*}\upsilon\left(\boldsymbol{r},t+\tau_{\upsilon}\right)\right] \tag{2.1.6}$$

We also consider a recently proposed non-Fourier heat conduction equation with a single delay term suggested by Quintanilla (2011). This heat conduction equation is developed as a reformulation of TPL heat conduction model (Roychoudhuri, 2007) by introducing a delay term between heat flux vector and thermal displacement vector with the assumption that the phase-lag of heat flux vector is equal to the phase-lag of the thermal gradient vector (i.e., $\tau_0=\tau_q-\tau_\upsilon$ and $\tau_q=\tau_T$). The heat conduction equation with a single time delay parameter is given by

$$q\left(\boldsymbol{r},t\right)=-\left[k\nabla T\left(\boldsymbol{r},t\right)+k^{*}\upsilon\left(\boldsymbol{r},t-\tau_{0}\right)\right] \tag{2.1.7}$$

The term τ_0 denotes the time delay parameter. The heat flux, temperature, and volumetric strain for an isotropic homogeneous thermoelastic body satisfy the relation (Guo, 2013)

$$-\nabla.q\left(r,t\right)=\rho C_{\upsilon}\frac{\partial T}{\partial t}+\frac{TE\alpha_{T}}{\left(1-2\nu\right)}\frac{\partial\epsilon}{\partial t} \tag{2.1.8}$$

From Eqs. (2.1.4)-(2.1.7), the unified heat conduction equation considering above four models can be expressed after taking a Taylor series expansion up to first order in τ_T

and τ_v, and up to second order in τ_q and τ_0 as follows

$$k^* \left[\nabla^2\theta + (\delta_{1j}\tau_v - \delta_{2j}\tau_0)\nabla^2\dot{\theta} + \frac{1}{2}\xi_0\tau_0^2\nabla^2\ddot{\theta}\right] + k\left[\nabla^2\dot{\theta} + \xi_1\tau_T\nabla^2\ddot{\theta}\right]$$
$$= \left[1 + (1+\delta_{3j})\,\xi_2\tau_q\frac{\partial}{\partial t} + \frac{1}{2}\delta_{1j}\tau_q^2\frac{\partial^2}{\partial t^2}\right]\left(\rho C_v\ddot{\theta} + \frac{T_0 E\alpha_T}{(1-2\nu)}\ddot{\epsilon}\right) \tag{2.1.9}$$

In above equation, ξ_0, ξ_1, and ξ_2 are dimensionless parameters introduced to consolidate all four models, and δ_{ij} is Kronecker delta. Above equation will be simplified to the respective heat conduction equations under four models as follows:

- LS model: $\tau_T = 0$, $\tau_q = 0$, $\tau_v = 0$, $\tau_0 = 0$.
- GN-III model: $\xi_0 = 0$, $\xi_1 = 1$, $\xi_2 = 1$, $j = 1$.
- TPL model: $k^* = 0$, $\xi_1 = 0$, $\xi_2 = \frac{1}{2}$, $j = 3$.
- Present model with single delay term: $\xi_0 = 1$, $\xi_1 = 0$, $\xi_2 = 0$, $j = 2$.

Assuming that the thermal gradients are much larger in the plane of the cross-section along the y-axis as compared to the gradients along the x-axis and there is no gradients exist along the z-axis, we can replace $\nabla^2\theta$ by $\frac{\partial^2\theta}{\partial y^2}$ in Eq. (2.1.9) to get

$$\left[\frac{k^*}{k}\left\{1 + (\delta_{1j}\tau_v - \delta_{2j}\tau_0)\frac{\partial}{\partial t} + \frac{1}{2}\xi_0\tau_0^2\frac{\partial^2}{\partial t^2}\right\} + \left(\frac{\partial}{\partial t} + \xi_1\tau_T\frac{\partial^2}{\partial t^2}\right)\right]\frac{\partial^2\theta}{\partial y^2}$$
$$= \frac{1}{\chi}\left[1 + (1+\delta_{3j})\,\xi_2\tau_q\frac{\partial}{\partial t} + \frac{1}{2}\delta_{1j}\tau_q^2\frac{\partial^2}{\partial t^2}\right]\left(\Gamma\ddot{\theta} - \frac{\triangle_E y}{\alpha_T}\frac{\partial^4 w}{\partial t^2\partial x^2}\right) \tag{2.1.10}$$

where $\Gamma = \frac{(1-2\nu)+2\triangle_E(1+\nu)}{(1-2\nu)}$, $\chi = \frac{k}{\rho C_v}$ is thermal diffusivity, and $\triangle_E = \frac{T_0 E\alpha_T^2}{\rho C_v}$ is the dimensionless parameter.

2.1.4 Solution for thermoelastic damping

In order to derive the expression of the inverse quality factor for TED, the solution of deflection and temperature in case of harmonic vibration can be assumed as (Lifshitz and Roukes, 2000)

$$w\left(x,t\right)=W_0\left(x\right)e^{i\omega t},\quad \theta\left(x,y,t\right)=\theta_0\left(x,y\right)e^{i\omega t} \tag{2.1.11}$$

where ω is angular frequency of vibration, W_0 is the displacement function, and θ_0 is temperature field function whose the imaginary part is out of phase with the real part of mechanical stresses. The amount of TED can be calculated in terms of the inverse of the quality factor as (Lifshitz and Roukes, 2000)

$$Q^{-1}=2\left|\frac{Im\left(\omega\right)}{Re\left(\omega\right)}\right| \tag{2.1.12}$$

From Eqs (2.1.10) and (2.1.11), one can obtain

$$\frac{\partial^2\theta_0}{\partial y^2}=\frac{\omega^2\left[\left(1-\frac{\tau_q^2}{2}\delta_{1j}\omega^2\right)+i\left(1+\delta_{3j}\right)\xi_2\tau_q\omega\right]}{\chi\left[\left\{\frac{k^*}{k}\left(1-\frac{\tau_0^2}{2}\xi_0\omega^2\right)-\xi_1\tau_T\omega^2\right\}+i\left\{\frac{k^*}{k}\left(\delta_{1j}\tau_\upsilon-\delta_{2j}\tau_0\right)+1\right\}\omega\right]}\left(-\Gamma\theta_0+\frac{\triangle_E y}{\alpha_T}\frac{\partial^2 W_0}{\partial x^2}\right) \tag{2.1.13}$$

The general solution of above equation is obtained as

$$\theta_0\left(x,y\right)=A_1 sin\left(p_1 y\right)+A_2 cos\left(p_1 y\right)+\frac{\triangle_E y}{\Gamma\alpha_T}\frac{\partial^2 W_0}{\partial x^2} \tag{2.1.14}$$

where A_1 and A_2 are arbitrary constants. The unknown parameter p in above equation is expressed as

$$p_1=\sqrt{\frac{\omega}{\chi}}\sqrt{a_1+ia_2}=\frac{\xi}{h}\left(\eta_1+i\frac{a_2}{|a_2|}\eta_2\right),\xi=h\sqrt{\frac{\omega}{2\chi}}$$

$$\eta_1=\sqrt{\sqrt{a_1^2+a_2^2}+a_1},\ \eta_2=\sqrt{\sqrt{a_1^2+a_2^2}-a_1}$$

$$a_1=\frac{\Gamma\omega\left[\frac{k^*}{k}-\left(\frac{k^*}{k}l_1+\xi_1\tau_T-\left(1+\delta_{3j}\right)\xi_2\tau_q\right)\omega^2+\frac{\tau_q^2}{2}l_2\delta_{1j}\omega^4\right]}{\left[\left\{\frac{k^*}{k}\left(1-\frac{\tau_0^2}{2}\xi_0\omega^2\right)-\xi_1\tau_T\omega^2\right\}^2+\left\{\frac{k^*}{k}\left(\delta_{1j}\tau_\upsilon-\delta_{2j}\tau_0\right)\omega+\omega\right\}^2\right]}$$

$$a_2 = \frac{\Gamma\omega\left[l_4\omega^3 - \frac{k^*}{k}l_3\omega - 1\right]}{\left[\left\{\frac{k^*}{k}\left(1 - \frac{\tau_0^2}{2}\xi_0\omega^2\right) - \xi_1\tau_T\omega^2\right\}^2 + \left\{\frac{k^*}{k}\left(\delta_{1j}\tau_\upsilon - \delta_{2j}\tau_0\right)\omega + \omega\right\}^2\right]}$$

$$l_1 = \tfrac{1}{2}\left(\tau_0^2\xi_0 + \tau_q^2\delta_{1j}\right) - \left(\delta_{1j}\tau_\upsilon - \delta_{2j}\tau_0\right)\left(1 + \delta_{3j}\right)\xi_2\tau_q$$

$$l_2 = \tfrac{k^*}{2k}\xi_0\tau_0^2 + \xi_1\tau_T$$

$$l_3 = \tfrac{\tau_q^2}{2}\delta_{1j}\delta_{2j}\tau_0 + \left(\delta_{1j}\tau_\upsilon - \delta_{2j}\tau_0\right) - \left(1 + \delta_{3j}\right)\xi_2\tau_q$$

$$l_4 = \tfrac{\tau_q}{2}\left[\left(\tfrac{k^*}{k}\delta_{1j}\tau_\upsilon + 1\right)\tau_q - \tfrac{k^*}{k}\left(1 + \delta_{3j}\right)\xi_0\xi_2\tau_0^2\right]$$

We assume that the boundaries of the resonator are adiabatic (Lifshitz and Roukes, 2000). Therefore, the boundary conditions are assumed to be

$$\frac{\partial\theta}{\partial y} = 0 \quad at \quad y = \pm\frac{h}{2} \tag{2.1.15}$$

From Eqs. (2.1.14) and (2.1.15), one can obtain

$$\theta_0\left(x, y\right) = \frac{\triangle_E y}{\Gamma\alpha_T}\left[y - \frac{sin\left(p_1 y\right)}{ycos\left(\frac{p_1 h}{2}\right)}\right]\frac{\partial^2 W_0}{\partial x^2} \tag{2.1.16}$$

Substituting Eqs. (2.1.11) and (2.1.16) into (2.1.3), we get

$$\begin{aligned} I &= \frac{bh^3}{12} \\ M_T &= \frac{\triangle_E I e^{i\omega t}}{\Gamma\alpha_T}\left[1 + \frac{12}{\left(p_1 h\right)^2} - \frac{24}{\left(p_1 h\right)^3}tan\left(\frac{p_1 h}{2}\right)\right]\frac{\partial^2 W_0}{\partial x^2} \end{aligned} \tag{2.1.17}$$

Substituting Eqs. (2.1.11) and (2.1.17) into Eq. (2.1.2), one can obtain

$$\omega^2 W_0 = \frac{EI}{\rho A}\left[1 + \frac{\triangle_E}{\Gamma}\left\{1 + f\left(\omega\right)\right\}\right]\frac{\partial^4 W_0}{\partial x^4} \tag{2.1.18}$$

where

$$f\left(\omega\right) = \frac{24}{\left(p_1 h\right)^3}\left[\frac{p_1 h}{2} - tan\left(\frac{p_1 h}{2}\right)\right] \tag{2.1.19}$$

On comparing Eq. (2.1.18) with the corresponding result of the normal mode of vibrations of the beam in the isothermal case, and by taking boundary conditions that the beam is clamped at both ends, we get

$$\omega = \omega_0 \sqrt{1 + \frac{\triangle_E}{\Gamma} \left\{1 + f\left(\omega\right)\right\}} \tag{2.1.20}$$

where $\omega_0 = q_n^2 \sqrt{\frac{EI}{\rho A}}$, $q_n = \frac{(2n+1)\pi}{2}$, $n = 1, 2, 3, ...$

Now, expanding the right-side of Eq. (2.1.20) with the help of Taylor series expansion in the power of $\triangle_E$ up to the first order, since $\triangle_E$ is very small, we obtain

$$\omega = \omega_0 \left[1 + \frac{\triangle_E}{\Gamma} \left\{1 + f\left(\omega\right)\right\}\right] \tag{2.1.21}$$

Since TED is very weak, therefore $f\left(\omega\right)$ can be replaced by $f\left(\omega_0\right)$ in above equation, and we arrive at the relation

$$\omega = \omega_0 \left[1 + \frac{\triangle_E}{\Gamma} \left\{1 + f\left(\omega_0\right)\right\}\right] \tag{2.1.22}$$

Using real and imaginary parts of above equation into Eq. (2.1.12), TED expression in terms of inverse quality factor is derived as

$$\begin{aligned} Q^{-1} = &\frac{24\triangle_E}{\Gamma} \left| \frac{a_2 \eta_1 \eta_2}{\left|a_2\right| \xi^2 \left(\eta_1^2 + \eta_2^2\right)^2} \right. \\ &- \left. \left\{ \frac{\frac{\eta_2}{\left|a_2\right|} a_2 \left(3\eta_1^2 - \eta_2^2\right) sin\left(\xi\eta_1\right) - \eta_1 \left(3\eta_2^2 - \eta_1^2\right) sin\left(\frac{\eta_2 \xi a_2}{\left|a_2\right|}\right)}{\xi^3 \left(\eta_1^2 + \eta_2^2\right)^3 \left(cos\left(\xi\eta_1\right) + cosh\left(\xi\eta_2\right)\right)} \right\} \right| \end{aligned} \tag{2.1.23}$$

2.1.5 Numerical results and discussion

This section is dedicated to illustrate the analytical results obtained in previous section and TED (Q^{-1}/Δ_E) of microbeam resonator made of silicon material with respect to the numerical values of the quality factor are investigated. We compare the nature of the variations of TED with respect to the beam height (h) and the normalized frequency

(ξ) predicted by the present thermoelastic model (Quintanilla, 2011). We also compare the results of this model with the corresponding results predicted by the thermoelastic models of type TPL, LS, and GN-III. Furthermore, we analyze the variation of TED for different aspect ratio (L/h). The material properties of silicon at reference temperature $293K$ are given below (Zenkour, 2016; Guo et al., 2016):

$E = 169\,GPa$, $\nu = 0.22$, $k = 156\,Wm^{-1}K^{-1}$, $\rho = 2330\,kg/m^3$, $C_v = 713\,J/kgK$, $\alpha_T = 2.6 \times 10^{-6}K^{-1}$, $k^* = 70\,Wm^{-1}K^{-1}s^{-1}$.

The thermal relaxation time τ_q quantitatively is expressed in terms of known parameters by Chester (1963) as follows:

$$\tau_q = \frac{3k}{\rho\varphi^2 C_v} \tag{2.1.24}$$

where φ is phonon velocity and it can be approximately replaced by the elastic wave velocity for the first vibration ($\varphi = 8433m/s$) (Francis, 1972). From (2.1.24), the approximate value of τ_q is found to be 0.0396×10^{-10}. The phase-lags τ_v and τ_T are considered here by the relations $\tau_v = 0.6\tau_q$ and $\tau_T = 0.7\tau_q$ (Quintanilla and Racke, 2008; Guo et al., 2016).

The variation of TED (Q^{-1}/Δ_E) versus normalized frequency ξ ($0 \leq \xi \leq 10$) and the thickness of the microbeam resonator $h\,(10^{-6} \leq h \leq 10^{-4})$ are displayed for different aspect ratios in the Figures 2.1.2 (a–c) and 2.1.3, respectively. Here, we consider $\tau_0 = \tau_q - \tau_v = 0.0158 \times 10^{-10}$.

Figure 2.1.2 (a–c) indicates the variations of TED with respect to normalized frequency ξ for aspect ratios 20, 25, and 30, respectively. The variations are shown for first mode, and it is clear that there exists a peak value of TED for each case under each model. The peak value of TED is different for TPL, GN-III , and LS models. However, in case of present and GN-III models, the peak values are noted to be the same. The quality factor is observed to be significantly different for TPL, LS, and new models, whereas there is no significant difference in the prediction by the present model and

GN-III model. It has been revealed that TED decreases with increase of aspect ratios of microbeam resonator predicted by TPL model and LS model while present model, and GN-III model have no effect on TED by changing aspect ratios. It can be seen that the difference in the peak value of TED decreases by increasing the aspect ratio of microbeam resonator.

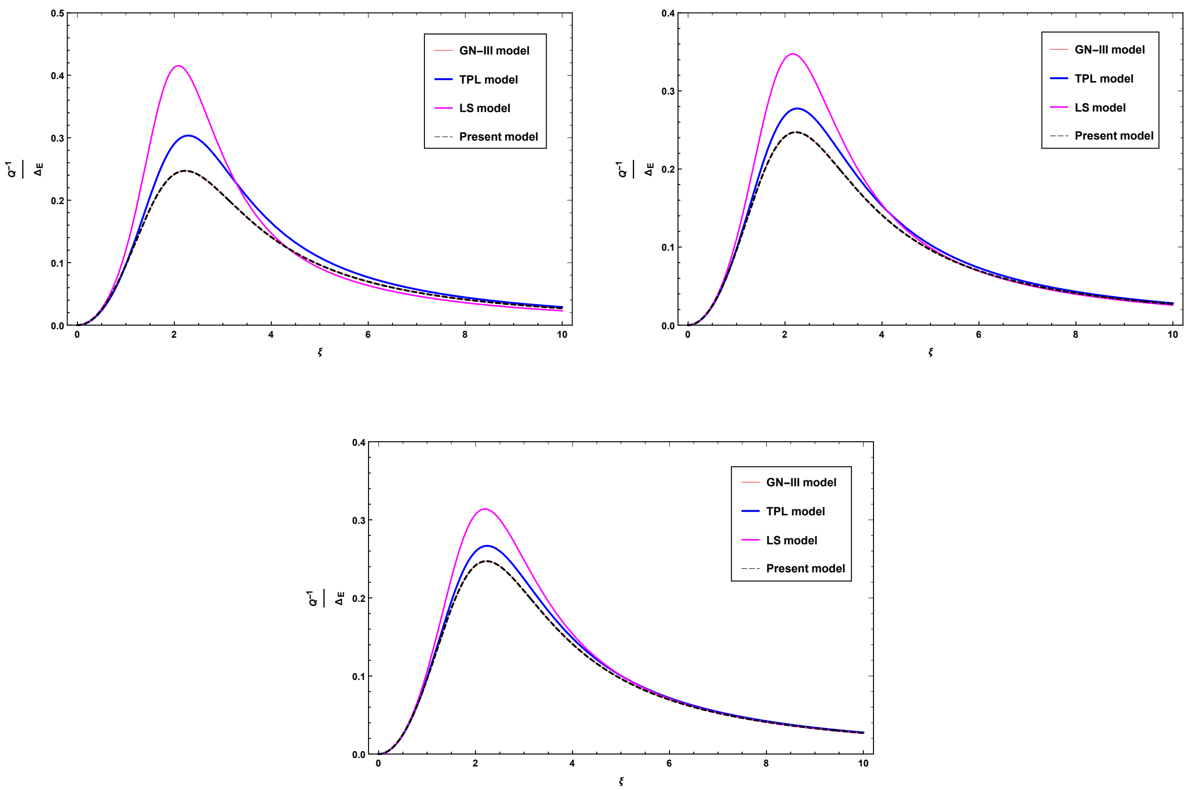

Figure 2.1.2: (a)Thermoelastic damping versus ξ for aspect ratio 20. (b) Thermoelastic damping versus ξ for aspect ratio 25. (c) Thermoelastic damping versus ξ for aspect ratio 30.

We note that present model predicts higher value of the quality factor in comparison to TPL and LS models, and the quality factor under this model agrees with the same under GN-III model. It has been further observed that the peak value of LS model is very sharp as compared to the value under TPL and present models. The TED curve of LS model first increases and after showing a maximum peak, it decreases and comes below the GN-III, TPL, and present model. It is clear that the quality factor of TED of beam resonator in context of LS and TPL models increases by increasing of aspect ratios implying that both of these models give high quality factor for large aspect ratios and energy dissipation during the vibration occurs more slowly.

Figure 2.1.3 shows the variation of TED with respect to microbeam thickness h ($10^{-6} \leq h \leq 10^{-4}$) for different aspect ratios 25 and 30. It is noted that the nature of vibrations of TED is the same for all thermoelastic models at microscale. It can be observed that the peak value of TED decreases by increasing of aspect ratio, and hence we find high quality factor for larger aspect ratios and the dissipation of energy is less during the vibrations. Therefore, oscillations will reduce more slowly and they will have a low level of damping. This implies that they will ring or vibrate for longer time. The effect of time delay parameter on the variation of TED as a function of normalized frequency is presented in Fig. 2.1.4. The graph is plotted for different values of time delay parameter (τ_0) by setting aspect ratio 25. From the Figure, it is clear that TED curve increases by increasing the value of time delay parameter. Moreover, the quality factor may be improved for small time delay.

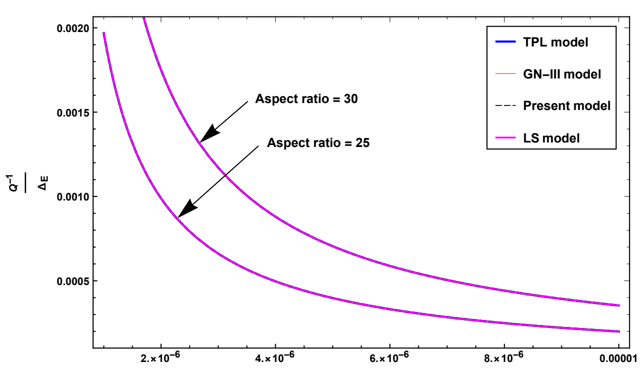

Figure 2.1.3: TED versus h for aspect ratios 25 and 30 under TPL, GN-III, LS, and present models.

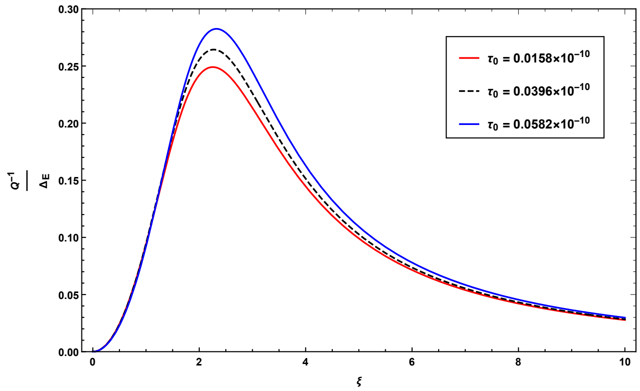

Figure 2.1.4: Effect of time delay parameter on TED versus normalized frequency for fixed aspect ratio 25.

2.1.6 Conclusion

In the present work, a combined expression for TED in terms of the inverse quality factor of the microbeam resonator has been derived under thermoelasticity theory based on Quintanilla, GN-III, TPL, and LS models. The complex frequency approach is used to obtain the expression for the quality factor. The effects of aspect ratios, normalized frequency, and beam thickness on TED of the microbeam resonator are discussed. The main observations of this investigation are highlighted as follows:

- The quality factor predicted by present model (Quintanilla model with a single delay term) is higher than the quality factor predicted by TPL and LS models.
- The results of present model mostly agree with the corresponding results under GN-III model.
- The quality factor of microbeam resonator increases with the decrease of beam thickness.
- The TED may be decreased for small time delay parameter.

2.2 Thermoelastic Damping in Nanobeam Resonators Utilizing Entropy Generation Approach and Heat Conduction Model with a Single Delay Term

2.2.1 Introduction[2]

It is worth to mention that as per the second law of thermodynamics, the heat flow can produce entropy, which appears as conversion of useful mechanical energy into heat. This process of entropy generation is used in the present subchapter of the thesis to discuss the results of thermoelastic damping in nanobeam resonators by employing the heat conduction theory with a single delay term. Kinra and Milligan (1994) analyzed TED based on the second law of thermodynamics and established a general theory for calculating TED from the entropy produced. Tai et al. (2014) developed an analytical model from the entropy generation equation and provided an accurate estimation of TED in flexural microbeam resonators. Zhou et al. (2019) investigated TED in micro and nanobeam resonators in the framework of generalized thermoelasticity with single-phase-lag time. Later on, Bostani and Mohammadi (2018) illustrated the behavior of TED in microbeam resonators using modified strain gradient elasticity as well as generalized thermoelasticity theory with one relaxation time. In their investigations, both frequency and entropy approach methods are used for finding the expressions of the quality factor.

Based on the previous works reported in the literature, the present section is devoted to illustrate TED in nanobeam resonators utilizing entropy generation approach method in the context of thermoelasticity equation with a single delay term proposed by Quintanilla (2011). In the previous subchapter of the thesis, it is observed that

[2]The content of this sub chapter is published in ***International Journal of Mechanical Sciences***, 165 (2020):105211.

for microbeam resonators, the TED and quality factor predicted by this new model is nearly the same with the prediction by GN-III model, however, it is significantly different as compared to the LS model and TPL model. Hence, this subsection of the thesis is attempted to investigate the quality factor of nanobeam resonators in the contexts of the Quintanilla model and GN-III model. An explicit expression of the quality factor for TED is derived. With the help of numerical results, the influence of TED in the context of normalized frequency as well as beam thickness is presented. The results of the present model are compared with those obtained for GN-III model. It has been observed that the current model offers a high quality factor of nanobeam as compared to GN-III model at nanoscale.

2.2.2 Problem formulation

The non-Fourier heat conduction equation with a single delay term given by Eq. (2.1.7) further can be written as

$$q_i\left(\boldsymbol{r},t\right)=-\left[kT_{,i}\left(\boldsymbol{r},t\right)+k^{*}\upsilon_{,i}\left(\boldsymbol{r},t-\tau_0\right)\right] \tag{2.2.1}$$

Expanding Eq. (2.2.1) up to second order in τ_0 by Taylor series expansion, one can obtain

$$q_i=-\left[\left(k-k^{*}\tau_0\right)T_{,i}+\frac{\tau_0^2k^{*}}{2}\dot{T}_{,i}+k^{*}\upsilon_{,i}\right] \tag{2.2.2}$$

Also, the equation (2.1.8) is further written as

$$-q_{i,i}=\rho C_v\frac{\partial T}{\partial t}+\frac{TE\alpha_T}{(1-2\nu)}\frac{\partial\epsilon}{\partial t} \tag{2.2.3}$$

By using Eqs. (2.2.2) and (2.2.3) in view of $\dot{\upsilon}=T$, we get

$$k^{*}T_{,ii}+\left(k-k^{*}\tau_0\right)\dot{T}_{,ii}+\frac{\tau_0^2k^{*}}{2}\ddot{T}_{,i}=\rho C_v\ddot{T}+\frac{TE\alpha_T}{(1-2\nu)}\ddot{\epsilon} \tag{2.2.4}$$

The above equation further can be rewritten in the following form

$$k^*\theta_{,ii} + (k - k^*\tau_0)\,\dot{\theta}_{,ii} + \frac{\tau_0^2 k^*}{2}\ddot{\theta}_{,i} = \rho C_v \ddot{\theta} + \frac{T_0 E \alpha_T}{(1-2\nu)}\ddot{\epsilon} \tag{2.2.5}$$

It is worth noting that when $\tau_0 = 0$, the present thermoelasticity model recovers the heat conduction equation under thermoelasticity theory of type GN-III.

2.2.3 TED in nanobeam resonators

We consider a very thin elastic beam (Euler-Bernoulli beam) with small flexural deflection of length L with a rectangular cross-section of dimension $h \times b$ as shown in Fig. 2.1.1, assuming the $x-$axis along the axis of the beam, $y-$axis along the thickness of the beam, and $z-$axis along the width of the beam. In the equilibrium, it is considered that the beam is unstrained, unstressed, and kept at uniform temperature T_0 everywhere. Inserting Eq. (2.1.1) into Eq. (2.2.5), one can obtain

$$\left[\frac{k^*}{k}\left(1 - \tau_0\frac{\partial}{\partial t} + \frac{\tau_0^2}{2}\frac{\partial^2}{\partial t^2}\right) + \frac{\partial}{\partial t}\right]\theta_{,ii} = \frac{1}{\chi}\left(\Gamma\ddot{\theta} - \frac{\Delta_E y}{\alpha_T}\frac{\partial^4 w}{\partial t^2 \partial x^2}\right) \tag{2.2.6}$$

It is further worth noting that thermal gradients in the cross-section of the plane along the $y-$direction are much larger than the gradients along the axis of beam and no gradient exists in the direction of $z-$axis. Therefore replacing $\theta_{,ii}$ by $\frac{\partial^2\theta}{\partial y^2}$ in Eq. (2.2.6), we obtain

$$\left[\frac{k^*}{k}\left(1 - \tau_0\frac{\partial}{\partial t} + \frac{\tau_0^2}{2}\frac{\partial^2}{\partial t^2}\right) + \frac{\partial}{\partial t}\right]\frac{\partial^2\theta}{\partial y^2} = \frac{1}{\chi}\left(\Gamma\ddot{\theta} - \frac{\Delta_E y}{\alpha_T}\frac{\partial^4 w}{\partial t^2 \partial x^2}\right) \tag{2.2.7}$$

2.2.4 Solution for harmonic vibration

To find the influence of thermoelastic coupling on harmonic vibrations of the beam resonator, the heat conduction equation Eq.(2.2.7) is solved for the case of harmonic vibrations. Substituting Eq. (2.1.11) into Eq. (2.2.7), we get

$$\left[\frac{k^*}{k}\left(1 - i\omega - \frac{\tau_0^2}{2}\omega^2\right) + i\omega\right]\frac{\partial^2\theta_0}{\partial y^2} = \frac{\omega^2}{\chi}\left(-\Gamma\theta_0 + \frac{\Delta_E y}{\alpha_T}\frac{\partial^2 W_0}{\partial x^2}\right)$$

$$\frac{\partial^2\theta_0}{\partial y^2} = -\frac{\omega^2}{\chi\left[\frac{k^*}{k}\left(1 - \frac{\tau_0^2}{2}\omega^2\right) + i\omega\left(1 - \frac{k^*\tau_0}{k}\right)\right]}\left(\Gamma\theta_0 - \frac{\Delta_E y}{\alpha_T}\frac{\partial^2 W_0}{\partial x^2}\right) \tag{2.2.8}$$

The general solution of the above equation can be obtained in the following form:

$$\theta_0\left(x, y\right) = B_1 sin\left(p_2 y\right) + B_2 cos\left(p_2 y\right) + \frac{\Delta_E y}{\Gamma\alpha_T}\frac{\partial^2 W_0}{\partial x^2} \tag{2.2.9}$$

where the unknown coefficients B_1 and B_2 are determined by applying thermal boundary conditions, and p can be expressed as:

$$p_2 = \sqrt{\frac{\omega}{\chi}}\sqrt{b_1 - ib_2} = \frac{\xi\eta}{h} - i\frac{\xi}{h\eta}b_2,\ \xi = h\sqrt{\frac{\omega}{2\chi}},\ \eta = \sqrt{b_1 + \sqrt{b_1^2 + b_2^2}}$$

$$b_1 = \frac{\Gamma\frac{k^*}{k}\left(1 - \frac{\tau_0^2}{2}\omega^2\right)\omega}{\left[\frac{k^*}{k}\left(1 - \frac{\tau_0^2}{2}\omega^2\right)\right]^2 + \left[\left(1 - \frac{k^*\tau_0}{k}\right)\omega\right]^2}$$

$$b_2 = \frac{\Gamma\left(1 - \frac{k^*\tau_0}{k}\right)\omega^2}{\left[\frac{k^*}{k}\left(1 - \frac{\tau_0^2}{2}\omega^2\right)\right]^2 + \left[\left(1 - \frac{k^*\tau_0}{k}\right)\omega\right]^2}$$

The thermal boundary conditions are taken such that the lower and upper surfaces of the beam are adiabatic. Therefore, in view of Eqs. (2.2.9) and (2.1.5), the temperature field function is obtained as:

$$\theta_0\left(x, y\right) = \frac{\Delta_E}{\Gamma\alpha_T}\frac{\partial^2 W_0}{\partial x^2}\left[y - \frac{sin\left(p_2 y\right)}{p_2\, cos\left(\frac{p_2 h}{2}\right)}\right] \tag{2.2.10}$$

2.2.5 Entropy based method for TED

The inverse of the quality factor can be defined in terms of energy loss and maximum stored energy per cycle of vibration as (Zener, 1938)

$$Q^{-1} = \frac{1}{2\pi}\frac{\Delta W}{W_{stored}} \tag{2.2.11}$$

where ΔW denotes the energy loss and W_{stored} denotes the maximum stored energy, respectively during one period of oscillation. Now, we aim to calculate the lost energy and the maximum stored energy during one period of oscillation. Firstly, the solution of Eq.(2.2.7) can be rewritten in the form of temperature field function as:

$$\theta\left(x, y, t\right) = \theta_0\left(x, y\right) sin\left(\omega t\right) \tag{2.2.12}$$

Here, ω is a real valued involved in the forced harmonic vibration with no attenuation during one period. From the second law of thermodynamic, the rate of entropy generation per unit volume is expressed as (Yourgrau, 2013)

$$\dot{s} = -\frac{1}{T^2} q_i T_{,i} \tag{2.2.13}$$

For simplification of this equation, when $\theta \ll 1$, the zeroth order term of the Taylor series expansion of T^{-2} around T_0 is considered as:

$$\frac{1}{T^2} = \frac{1}{T_0^2} - O\left(\frac{2}{T_0^3}\theta\right) \tag{2.2.14}$$

Hence, substituting the values of q_i from Eq. (2.2.13) into Eq. (2.2.2) and then using Eq. (2.2.14), we arrive at the relation

$$\ddot{s} + \left(\frac{2\dot{T}}{T_0} - \frac{\dot{T}_{,i}}{T_{,i}}\right)\dot{s} = \left[k^* + \left(k - k^*\tau_0\right)\frac{\partial}{\partial t} + \frac{\tau_0^2 k^*}{2}\frac{\partial^2}{\partial t^2}\right]\frac{\left(T_{,i}\right)^2}{T_0^2} \tag{2.2.15}$$

Since, the term $\frac{2\dot{T}}{T_0}$ is small, hence for mathematical simplicity neglecting this term in Eq. (2.2.15) , therefore the solution of Eq. (2.2.15) for $\dot{s}$ is acquired as:

$$\dot{s} = \frac{1}{T_0^2}\left(\frac{\partial\theta_0}{\partial y}\right)^2\left[\left(\frac{k-k^*\tau_0}{\omega^2}\right)sin^2\left(\omega t\right)-\frac{k^*}{2\omega}\left(1-\frac{\tau_0^2}{2\omega^2}\right)sin\left(2\omega t\right)\right] \tag{2.2.16}$$

Inserting Eq. (2.2.10) into Eq. (2.2.16), one can obtain

$$\dot{s} = \frac{1}{T_0^2}\left(\frac{\Delta_E}{\Gamma\alpha_T}\frac{\partial^2 W}{\partial x^2}\right)^2\left[1-\frac{cos\left(p_2 y\right)}{cos\left(\frac{p_2 h}{2}\right)}\right]^2\left\{sin^2\left(\omega t\right)-\frac{k^*}{k}\frac{sin\left(2\omega t\right)}{2\omega}\right\} \tag{2.2.17}$$

The generation of entropy per unit volume over one cycle of vibration is given by

$$\Delta s = \oint \dot{s}dt \tag{2.2.18}$$

By using Eqs. (2.2.17) and (2.2.18), we obtain

$$\Delta s = \frac{\pi}{\omega^3}\frac{\left(k-k^*\tau_0\right)}{T_0^2}\left(\frac{\Delta_E}{\Gamma\alpha_T}\frac{\partial^2 W_0}{\partial x^2}\right)^2\left[1-\frac{cos\left(p_2 y\right)}{cos\left(\frac{p_2 h}{2}\right)}\right]^2 \tag{2.2.19}$$

We can obtain the total entropy production over one cycle by integrating Eq. (2.2.19) over the volume of the beam as follows:

$$\Delta S = \int_V \Delta s dV \tag{2.2.20}$$

Substituting Eq. (2.2.19) into Eq. (2.2.20), we find the following expression

$$\Delta S = \frac{\pi}{\omega^3}\frac{\left(k-k^*\tau_0\right)\Delta_E^2 h}{\alpha_T^2 T_0^2\Gamma^2}\widetilde{A}.\widetilde{B} = \frac{\pi\left(1-\frac{k^*\tau_0}{k}\right)h^3 E\Delta_E}{2\Gamma^2 T_0\xi^2}\widetilde{A}.\widetilde{B} \tag{2.2.21}$$

where $\widetilde{A}$ and $\widetilde{B}$ are the complex functions given by

$$\begin{aligned}\widetilde{A} &= \int_{-\frac{h}{2}}^{+\frac{h}{2}} \left[1 + \frac{cos^2\left(p_2 y\right)}{cos^2\left(\frac{p_2 h}{2}\right)} - \frac{2cos\left(p_2 y\right)}{cos\left(\frac{p_2 h}{2}\right)}\right] dy \\ &= 1 + \frac{1}{1 + cos\left(p_2 h\right)} - \frac{3}{p_2 h} tan\left(\frac{p_2 h}{2}\right)\end{aligned} \tag{2.2.22}$$

$$\widetilde{B} = \int_0^L \int_{-\frac{b}{2}}^{+\frac{b}{2}} \left(\frac{\partial^2 W_0}{\partial x^2}\right)^2 dz dx = b \int_0^L \left(\frac{\partial^2 W_0}{\partial x^2}\right)^2 dx \tag{2.2.23}$$

The real and imaginary parts of Eq. (2.2.22) can be separated in view of $p_2 = \frac{\xi \eta}{h} - i \frac{\xi}{h\eta} b_2$ as follows:

$$Re\left(\widetilde{A}\right) = 1 + \frac{1 + cos\left(\xi\eta\right) cosh\left(\frac{\xi b_2}{\eta}\right)}{\left[cos\left(\xi\eta\right) + cosh\left(\frac{\xi b_2}{\eta}\right)\right]^2} - \frac{3\eta\left(\eta^2 sin\left(\xi\eta\right) + b_2 sinh\left(\frac{\xi b_2}{\eta}\right)\right)}{\xi\left(\eta^4 + b_2^2\right)\left[cos\left(\xi\eta\right) + cosh\left(\frac{\xi b_2}{\eta}\right)\right]}$$

$$Im\left(\widetilde{A}\right) = -\frac{sin\left(\xi\eta\right) sinh\left(\frac{\xi b_2}{\eta}\right)}{\left[cos\left(\xi\eta\right) + cosh\left(\frac{\xi b_2}{\eta}\right)\right]^2} - \frac{3\eta\left(b_2 sin\left(\xi\eta\right) - \eta^2 sinh\left(\frac{\xi b_2}{\eta}\right)\right)}{\xi\left(\eta^4 + b_2^2\right)\left[cos\left(\xi\eta\right) + cosh\left(\frac{\xi b_2}{\eta}\right)\right]}$$

Therefore, the total dissipated energy ΔW can be calculated as:

$$\Delta W = T_0 \left|\Delta S\right| = \frac{\pi\left(1 - \frac{k^* \tau_0}{k}\right) h^3 E \Delta_E \widetilde{B}}{2\Gamma^2 \xi^2} \sqrt{Re\left(\widetilde{A}\right)^2 + Im\left(\widetilde{A}\right)^2} \tag{2.2.24}$$

Further, the maximum stored energy W_{stored} over entire beam per cycle is given by

$$W_{stored} = \frac{1}{2} \int\limits_V \sigma_{xx} \epsilon_{xx} dV \tag{2.2.25}$$

where $\sigma_{xx} = E\epsilon_{xx}$. Therefore, the maximum stored energy from above equation is obtained as:

$$W_{stored} = \frac{Ebh^3}{24} \int_0^L \left(\frac{\partial^2 W_0}{\partial x^2}\right)^2 dx = \frac{Eh^3 \widetilde{B}}{24} \tag{2.2.26}$$

Now, using Eqs. (2.2.24) and (2.2.26) into Eq. (2.2.11), the expression for the inverse quality factor to calculate TED in beam resonators is finally derived as:

$$Q^{-1} = \frac{6\left(1-\frac{k^*\tau_0}{k}\right)\Delta_E}{\Gamma^2\xi^2}\left[\left\{1+\frac{1+cos\left(\xi\eta\right)cosh\left(\frac{\xi b_2}{\eta}\right)}{\left[cos\left(\xi\eta\right)+cosh\left(\frac{\xi b_2}{\eta}\right)\right]^2}-\frac{3\eta\left(\eta^2 sin\left(\xi\eta\right)+b_2 sinh\left(\frac{\xi b_2}{\eta}\right)\right)}{\xi\left(\eta^4+b_2^2\right)\left[cos\left(\xi\eta\right)+cosh\left(\frac{\xi b_2}{\eta}\right)\right]}\right\}^2\right.$$
$$\left.+\left\{\frac{sin\left(\xi\eta\right)sinh\left(\frac{\xi b_2}{\eta}\right)}{\left[cos\left(\xi\eta\right)+cosh\left(\frac{\xi b_2}{\eta}\right)\right]^2}+\frac{3\eta\left(b_2 sin\left(\xi\eta\right)-\eta^2 sinh\left(\frac{\xi b_2}{\eta}\right)\right)}{\xi\left(\eta^4+b_2^2\right)\left[cos\left(\xi\eta\right)+cosh\left(\frac{\xi b_2}{\eta}\right)\right]}\right\}^2\right]^{\frac{1}{2}} \tag{2.2.27}$$

2.2.6 Numerical results and discussion

In the previous section, the explicit formula of the quality factor for TED of nanobeam resonator is derived as Q^{-1}/Δ_E by applying the entropy generation approach. The present work aims to investigate the TED in nanobeam resonators based on the modified heat conduction equation with a single delay term proposed by Quintanilla (2011). The results of the present model are compared to the corresponding results of the thermoelasticity theory of type GN-III. The effects of some parameters on the TED such as aspect ratio, beam thickness, and dimensionless frequency, are studied. Furthermore, the effects of material constant k^* (conductivity rate) on the quality factor for TED is also discussed. Here, the material of the beam is selected as silicon. The properties of silicon material are listed below (Li et al., 2012):

$T_0 = 293\,K,\ E = 169\,GPa,\ \rho = 2330\,Kg/m^3,\ \nu = 0.22,\ k = 156\,W/mK,\ C_v = 1.64\times10^6\,J/mK,\ \alpha_T = 2.6\times10^{-6}\,K^{-1}$ and we take the value of the delay time parameter as $\tau_0 = 1.72\times10^{-12}s$.

Figures 2.2.1 $-$ 2.2.3 show the variation of thermoelastic damping Q^{-1}/Δ_E (scaled by the relaxation strength Δ_E) with dimensionless frequency, ξ for various aspect ratios in the contexts of the present model and GN-III model. We show the results for the cases when the aspect ratio $L/h = 25$ and $L/h = 30$. Figs. $2.2.1 - 2.2.3$ also depict the effects of the material parameter (conductivity rate), k^* on TED. This parameter is the characteristic of the present model and GN-III model. In the graphs, two curves show the results for TED associated with GN-III model and the present thermoelasticity model involving a single delay term parameter. As shown in these Figures, the method based on entropy generation is almost close to the curve of the GN-III model for the high-frequencies range.

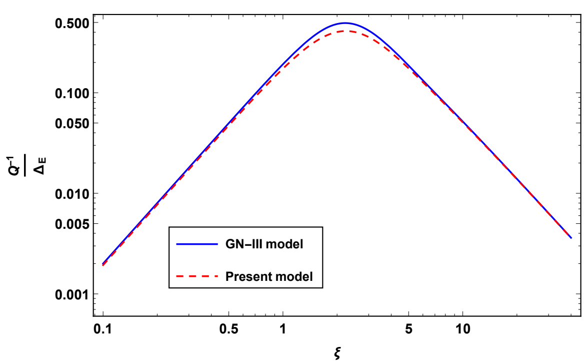

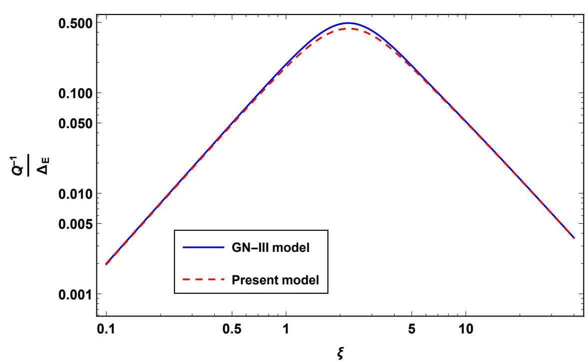

Figure 2.2.1: Variation of Q^{-1}/Δ_E versus non-dimensional frequency ξ for fixed $k^* = 90$ and aspect ratio (a) $L/h = 25$ and (b) $L/h = 30$.

In the case of both the models, the peak value of TED occurs nearly for $\xi \simeq 2.224$. It has been observed that TED increases to a maximum peak value as the frequency increases and decreases after reaching the peak value. The peak value is for the configuration on which the lost energy is the highest. It can be concluded that the difference between the prediction of quality factor by two models decreases as we increase the aspect ratio of the beam. Therefore, for large aspect ratio, the quality factor is almost the same for both the models. Furthermore, for large frequencies with a fixed aspect ratio L/h , the errors are negligible. It is further observed that the present model offers the high-quality factor for small aspect ratio in comparison to GN-III model. From the Figures, the effects of material constant k^* on TED can be observed to be very much prominent, implying that there is a significant difference in the prediction of quality factor by the present model as compared to the GN-III model. When the material constant k^* is smaller than thermal conductivity k, the Q-factor decreases, and when it is greater or equal to k, the quality factor increases from GN-III model. In all cases, the results of the quality factor for TED obtained by the present model are better than those shown by GN-III model.

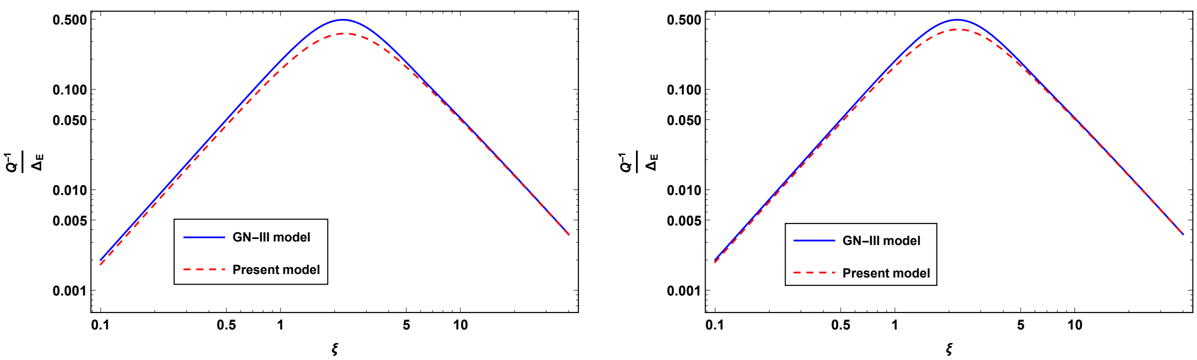

Figure 2.2.2: Variation of Q^{-1}/Δ_E versus non-dimensional frequency ξ for fixed $k^* = 156$ and aspect ratio (a) $L/h = 25$ and (b) $L/h = 30$.

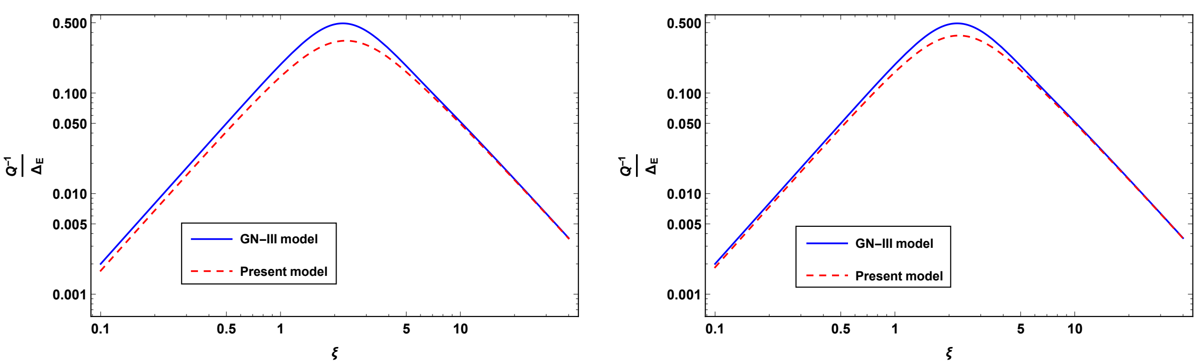

Figure 2.2.3: Variation of Q^{-1}/Δ_E versus non-dimensional frequency ξ for fixed $k^* = 200$ and aspect ratio (a) $L/h = 25$ and (b) $L/h = 30$.

Figures 2.2.4$(a - c)$ display the variation of thermoelastic damping Q^{-1}/Δ_E (scale by the relaxation strength Δ_E) for different aspect ratios ($L/h = 25$ and $L/h = 30$) of the beam with respect to thickness at nanometer scale. From these figures, one can also observe the effects of material constant k^* on TED. Here, we have considered three cases i.e., when $k^* < k$, $k^* = k$, and $k^* > k$. It is noticed that the difference of peak value in the quality factor is larger for smaller aspect ratio associated with present and GN-III models. Also, with the increase of aspect ratio, the peak value decreases. From these Figures, it is clear that when we increase aspect ratio, the value of the quality factor decreases.

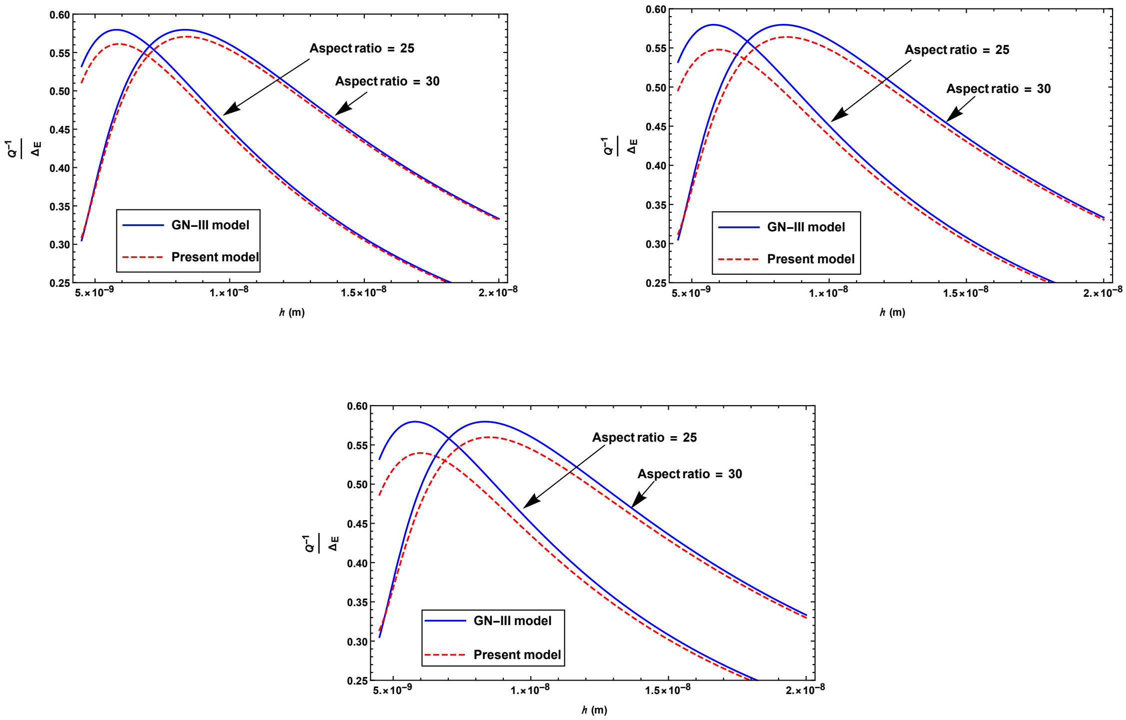

Figure 2.2.4: Variation of Q^{-1}/Δ_E versus beam thickness h for (a) $k^* = 90$, (b) $k^* = 156$, and (c) $k^* = 200$.

Furthermore, it is found that the value of the quality factor in present model is greater than the quality factor under GN-III model and hence, a lower rate of energy loss relative to the stored energy of the resonator can be achieved by applying the present new model. Therefore, this nano resonator with high-quality factor has low damping so that they ring or vibrate for longer duration of time. As observed from Figure 2.2.4$(a - c)$, when we increase the value of material constant k^*, TED decreases and hence, in this case, we can obtain high-value of the quality factor of the beam resonator. However, the present model offers high quality factor at nanometer scale. This is believed to be an important observation of the present study.

2.2.7 Conclusion

The present work demonstrates the prediction of the quality factor of TED in nanobeam resonators on the basis of the heat conduction model with a single delay term proposed by Quintanilla (2011). To derive the expression of the inverse quality factor for TED, the entropy generation approach method has been used. The quality factor is obtained by calculating the energy dissipated per cycle of vibration over the volume of the beam resonator. The influences of beam thickness, aspect ratio, and dimensionless frequency on the quality factor for TED are investigated in a detailed way. Furthermore, the effects of material constant k^* (conductivity rate) on TED is also discussed. The results of the present model are compared to the corresponding results obtained for GN-III model. The main highlights from the present investigation are outlined as follows:

- The prediction of the quality factor by the present model is higher as compared to the prediction by GN-III model at nanoscale.
- The higher value of the quality factor of the present model as compared to the GN-III model can be observed only at the nanoscale, while the quality factor remains approximately the same as GN-III model at the microscale.
- For small-sized beams, the quality factor of nanobeam can be enhanced.
- The high-quality factor can also be obtained for higher values of the material constant, k^*.